Re-submitted to: *Chemosphere* (**CHEM 17563**)

Date: 26 November 2009

Fate of aerobic bacterial granules with fungal contamination under different organic loading conditions

An-jie Li, Tong Zhang and Xiao-yan Li*

Environmental Engineering Research Centre, Department of Civil Engineering,

The University of Hong Kong, Pokfulam Road, Hong Kong, China

*Corresponding Author:

Phone: (852) 2859-2659
Fax: (852) 2559-5337
Email: xlia@hkucc.hku.hk
Homepage: http://web.hku.hk/~xlia/

Running Head: Special aerobic sludge granules

Abstract

Aerobic sludge granulation is an attractive new technology for biological wastewater treatment. However, the instability of aerobic granules caused by fungal growth is still one of the main problems encountered in granular bioreactors. In this study, laboratory experiments were conducted to investigate the fate and transformation of aerobic granules under different organic loading conditions. Bacterial granules (2-3 mm) in a poor condition with fungi-like black filamentous growth were seeded into two 1-L batch reactors. After more than 100 d of cultivation, the small seed granules in the two reactors had grown into two different types of large granules (> 20 mm) with different and unique morphological features. In reactor R1 with a high organic loading rate of 2.0 g COD L^{-1} d^{-1}, the black filaments mostly disappeared from the granules, and the dominance of rod-shaped bacteria was recovered. In contrast, at a low loading of 0.5 g COD L^{-1} d^{-1} in reactor R2, the filaments eventually became dominant in the black fungal granules. The bacteria in R1 granules had a unique web-like structure with large pores of a few hundred μm in size, which would allow for effective substrate and oxygen transport into the interior of the granules. DNA-based molecular analysis indicated the evolution of the bacterial population in R1 and that of the eukaryal community in R2. The experimental results suggest that a high loading rate can be an effective means of helping to control fungal bloom, recover bacterial domination and restore the stability of aerobic granules that suffer from fungal contamination.

Keywords: Aerobic granulation; bacterial granules; biological wastewater treatment; FISH-CLSM; fungal granules; PCR-DGGE.

1. Introduction

The granulation of aerobic sludge in a sequencing batch reactor (SBR) is an attractive new technology for biological wastewater treatment. It is characterised by an excellent sludge settling rate, great biomass enrichment, a low sludge yield, nitrogen removal and fast start-up compared to anaerobic granulation (Morgenroth et al., 1997; Arrojo et al., 2004; Qin and Liu, 2006). However, one of the main problems encountered in the operation of a granular sludge SBR is the instability of the aerobic granules. Filamentous growth, or fungal bloom, has often been observed on such granules (Tay et al., 2001; Schwarzenbeck et al., 2005). Once filamentous growth dominates the reactor, the granules begin to deteriorate in quality and settleability, which leads to subsequent biomass washout and the eventual failure of the granular system. Hence, the instability and deterioration of aerobic granules is a major concern in the application of aerobic granulation technology in wastewater treatment.

Filamentous bacterial and fungal species have been implicated in the structural development of granules (Beun et al., 1999; Weber et al., 2007; Yang et al., 2008). Liu and Tay (2004) reported that the structure and species diversity of granules may be related to the type of carbon source. In their study, glucose-fed aerobic granules exhibited a loose morphology and were dominated by filamentous bacteria, whereas acetate-fed aerobic granules had a compact structure and were dominated by rod-shaped bacteria with little filamentous growth. However, other studies have shown that a filamentous structure is not necessary for the formation of glucose-fed aerobic granules and that these granules still have a compact structure dominated by rod-shaped bacteria (Li et al., 2008a; Yang et al., 2008). However, a low-pH glucose-based growth medium may lead to the formation of filamentous fungal granules (Yang et al., 2008). Thus, the factors that encourage filamentous growth during aerobic granulation remain unclear, and the types and properties of filamentous microorganisms that affect the structural features and microbial communities of aerobic

granules need to be investigated. Effective measures for controlling the filamentous species in granules and recovering granules that suffer from filamentous growth remain to be developed.

Filamentous microorganisms, including fungi, are commonly slow-growing species compared to non-filamentous bacteria. It has been reported that the settling problems of activated sludge that result from excessive filamentous growth always appear in wastewater treatment plants that have a low organic loading rate (Knoop and Kunst, 1998). Filamentous growth has also been observed in a granular sludge SBR under conditions of a high biomass concentration or a low substrate loading rate (Liu et al., 2005). Filamentous species have an advantage over non-filamentous species in granules, as they are able to take up more nutrients from media with a low level of nutrients (Liu and Liu, 2006). As noted by Eckenfelder (2000), the growth of filamentous species is favoured in substrates at a low concentration. Hence, the organic loading rate can be an important factor in the control of filamentous bloom and in the recovery of granules having the problem of filamentous growth.

In the experimental study reported herein, aerobic sludge granules cultivated in a SBR were placed as seed granules into two batch reactors with two different organic loading rates. These seed bacterial granules had already begun to deteriorate in quality with fungi-like black filamentous growth on their surface. The changes in the morphology, structure and microbial community of the granules under different growth conditions were characterised via scanning electron microscopy (SEM), confocal laser scanning microscopy (CLSM), fluorescence in-situ hybridisation (FISH) and CLSM observation, microbial DNA extractions followed by polymerase chain reactions (PCR), denaturing gradient gel electrophoresis (DGGE) and clone library analysis. The aim of the study was to investigate the fate of aerobic granules with filamentous contamination under different substrate loading conditions and to evaluate the operating measures for the recovery and improvement of the stability of such granules.

2. Materials and methods

2.1. Experimental set-up and operation

Two 1 L glass beakers (H 11 cm × D 11 cm) were used as batch reactors for the granule growth experiment. Small granules of 2-3 mm in diameter collected from a laboratory SBR were placed as seed granules into the two batch reactors, R1 and R2. These seed granules, which are used to treat glucose-based synthetic wastewater, were typical yellow-coloured bacterial granules. However, the granules had begun to deteriorate in quality with apparent black fungal growth on their surface (Figs. 1a and 1b). The initial suspended solids (SS) concentration of the seed granules in the two batch reactors was 1 g L^{-1}. The reactors were fed once a day, after effluent withdrawal, with a substrate solution that consisted of glucose and other nutrients (Tay et al., 2002; Li et al., 2008a). The operating conditions for the two reactors were the same except for the feeding substrate concentration. Two different organic concentrations in terms of chemical oxygen demand (COD) - 2000 and 500 mg L^{-1} - were used for R1 and R2, resulting in COD loading rates of 2.0 g L^{-1} d^{-1} (R1) and 0.5 g L^{-1} d^{-1} (R2), respectively. $NaHCO_3$ was dosed into the feed solution to maintain the pH of the reactors in the neutral range between 7.0 and 7.5. Aeration was supplied through an air diffuser at the bottom of each reactor, and the dissolved oxygen (DO) concentration in the sludge suspension was about 5 mg L^{-1}. The reactors were operated at room temperature, and the water temperature was 20-22 ˚C.

2.2. Analytical methods

The COD and SS concentrations were measured according to Standard Methods (APHA, 1998). The DO concentration was determined with a DO probe (5010 BOD Probe, YSI) and

a DO meter (5000 DO meter, YSI), and the pH was measured with a pH meter (420A, Orion). The morphology of the aerobic granules was observed under a stereomicroscope (S8 APO, Leica, Wetzlar, Germany) equipped with a digital camera (EC3, Leica). A digital camera (Kodak V530, Kodak, Rochester, NY, USA) was also used to take photographs of the large granules for characterisation. The projected images of the granules were analysed for their sizes and surface roughness using a computer-based image analysis system (AnalySIS 3.1, Olympus Soft Imaging Solutions, Germany). The roughness of a granule was determined from the ratio between the actual boundary of the granule image and the perimeter of a circle that covers the same area of the granule. In addition, the microstructure of the mature granules was examined under SEM (Cambridge S440, Oxford Instruments, Cambridge, UK) following the sample pre-treatment detailed by Diao et al. (2004) and Chu and Li (2005). The total organic carbon (TOC) concentration was measured using a TOC analyser (IL550, HACH-Lachat, Milwaukee, WI, USA).

2.3. FISH and CLSM examinations

The 3-D structure of the mature granules, particularly the distributions of the microbial cells and extracellular polymeric substances (EPS) within the granules, was examined via CLSM (LSM 5 Pascal, Zeiss, Jena, Germany) following the procedures described in previous studies (Zhang and Fang, 2004; Yang et al., 2008). In brief, for the fluorescent staining of the cells and EPS, two probes were applied together: SYTO9 (25 μM, Molecular Probe) to target all of the microbes and ConA-TRITC lectin (250 mg L^{-1}, Sigma) to target the polysaccharides. When excited by a laser at proper wavelengths, SYTO9 and ConA-TRITC probes emit green and red light, respectively. For sample preparation, a granule was embedded in Tissue-Tek OCT Compound (Miles, Elkhart, IN, USA) and frozen overnight at -20 °C. This frozen granule was sectioned into thicknesses of 50 μm using a rotary cryo-microtome (CM 1510-

123 Cryostat, Leica, Germany), and the section specimens were then stained and examined under
124 CLSM.

125 In addition, the bacterial and fungal cells in the mature granules were distinguished via
126 FISH with specific probes for an estimation of their relative abundance. A sample with a few
127 granules was homogenised with a beadbeater (Mini-beadbeater, Biospec, Bartlesville, OK,
128 USA) without beads, and the microbial cells were suspended with a vortex mixer. The cell
129 suspension was fixed using paraformaldehyde (4%) and then placed onto a microscopic slide.
130 FISH staining was conducted at 20% formamide using fluorescein isothiocyanate (FITC) -
131 labelled probe Eub338 (5'-GCTGCCTCCCGTAGGAGT-3') for the bacteria (green) and
132 Cy3-labelled probe Euk516 (5'-ACCAGACTTGCCCTCC-3') for the fungi (red). The FISH-
133 CLSM images of the cells after staining were processed with an image analysis system
134 (LSM5 Pascal, V2.8 SP1, Zeiss, Jena, Germany). The relative abundance of the bacteria and
135 fungi in the granules was estimated based on the total projected areas of the bacterial and
136 fungal cells, respectively.

137

138 *2.4. DNA extraction, PCR-DGGE and microbial species identification*

139 The genomic DNA of the biomass was extracted from the granules following the protocol
140 described by Zhuang et al. (2005) using a beadbeater (Mini-beadbeater, Biospec, Bartlesville,
141 OK, USA) and a micro-centrifuge (MiniSpin plus, Eppendorf, Hamburg, Germany). The
142 extracted DNA was then used as the template for PCR amplification. For the bacterial species,
143 the variable V3 region of the 16S rDNA was amplified using primers 341f-GC and 518r
144 (Muyzer et al., 1993) with a DNA Engine Peltier Thermal Cycler (PTC-200, MJ Research,
145 Waltham, MA, USA) following a touchdown thermal profile (Watanabe et al., 1998). For the
146 eukaryal species, primers Euk1A and Euk516r-GC were used in the PCR programme.
147 Amplification began with initial denaturation at 94 °C for 130 s, followed by 35 cycles of

denaturation at 94 °C for 30 s, annealing at 56 °C for 45 s and extension at 72 °C for 130 s. It ended with a final elongation step at 72 °C for 7 min (Diez et al., 2001).

The PCR-amplified DNA products were separated via DGGE, and the DGGE images were acquired using the ChemiDoc (Bio-Rad, Hercules, CA, USA) gel documentation system. For bacterial DNA, the samples were run on 8% polyacrylamide gels in a linear gradient with a 30-50% denaturing condition at 130 v for 6 h at 60 °C. For eukaryal DNA, the samples were run in a gradient with a 20-40% denaturing condition at 100 v for 16 h at 60 °C. The DGGE gels were scanned and the scanned images were analysed for the band patterns using the Quantity One 1-D analysis software (Bio-Rad). The relative abundance of the possible species in a sludge sample was determined from its DGGE gel image based on the peak value of the band brightness.

To identify the phylogeny of the bacterial DGGE bands, a 16S rRNA gene clone library was constructed. PCR was performed using universal bacterial primers 27f and 1495r, according to the programme used by Liu et al. (2006). The PCR products, which were approximately 1450 bps long, were purified using a DNA gel extraction kit (MEGA-spin, iNtRON *Biotechnology*, Korea). The purified PCR products were then cloned into *Escherichia coli* TOP10 using the pCRII-TOPO vector system (Invitrogen, Carlsbad, CA, USA). A total of 98 recombinant clones were selected randomly for plasmid recovery and analysis, and the extraction and sequencing of the plasmids were carried out by a commercial laboratory (Tech Dragon, http://www.techdragon.com.hk/index.htm). All of the sequences obtained were compared with the 16S rRNA gene sequences in the GenBank using a BLAST search (National Center for Biotechnology Information, U.S. National Library of Medicine) for identification of the closest bacterial species.

Each band on the DGGE profile was defined as an operational taxonomic unit (OTU). Representative plasmids in the clone library were used to perform DGGE together with the

PCR products of the DNA from the granules. Based on the migration position, the sequence of a plasmid and its closest species known in the clone library was assigned to an OTU (particular band) in the DGGE profile of the granule sample. A small number of DGGE bands, which had no matching plasmids in the clone library, was sliced out, purified, re-amplified and sequenced. These sequences were then analysed with an ABI PRISM 3700 DNA Analyser (Applied Biosystems, Foster City, CA, USA) for species identification (Li et al., 2008a).

To identify the eukaryal species in the granules, the DGGE bands were cut off from the gels, purified and re-amplified using the same PCR procedures as those used for eukaryal DNA. The PCR products were sequenced with BigDye Terminator Reactions (ABI PRISM BigDye Terminators V3.1 Kit, Applied Biosystems, Foster City, CA, USA) and the ABI PRISM 3700 DNA Analyser. The sequences were analysed by comparing them with the 18S rRNA gene sequences in the GenBank by a BLAST search to identify the fungi and other eukaryal species.

2.5. Accession Numbers

The DNA sequences obtained in this study were deposited in GenBank and were assigned accession numbers FJ588654-FJ588680.

3. Results

3.1. Formation of different types of aerobic granules in the two reactors

The seed aerobic granules collected from a granular sludge SBR already showed signs of deterioration. Most of these yellow bacterial granules were partially covered with a fungi-like black filamentous growth (Figs. 1a and 1b). Small granules were cultivated under a high

organic loading (2.0 g COD L^{-1} d^{-1}) condition in reactor R1 and under a low organic loading (0.5 g COD L^{-1} d^{-1}) condition in reactor R2. The resulting initial food-to-microorganism (F/M) ratios were 2.0 g COD g^{-1} SS d^{-1} in R1 and 0.5 g COD g^{-1} SS d^{-1} in R2. After 120 d, the granules in the two reactors had both become much larger, but had grown into two different types of microbial entities with entirely different and unique morphological features (Figs. 1c and 1d). More importantly, the large granules in R1 were recovered as bacterial granules with a smooth and yellow surface, whilst those in R2 appeared to be puffy balls of black fungal filaments. The sludge SS concentration increased gradually from 1 to 2.5 g L^{-1} for both reactors during the growth process. Accordingly, the F/M ratio decreased to around 0.8 g COD g^{-1} SS d^{-1} in R1 and about 0.2 g COD g^{-1} SS d^{-1} in R2. Both reactors performed well in wastewater treatment with an effluent COD of less than 100 mg L^{-1} from R1 and less than 60 mg L^{-1} from R2, corresponding to organic removal efficiencies of 95% (R1) and 88% (R2).

The large granules in R1 ranged from 12 to 21 mm in diameter, and those in R2 from 20 to 35 mm. The R1 granules had a smooth surface with a roughness value of 1.03±0.05, which was much lower than the roughness value of 1.84±0.08 amongst the R2 granules. Despite their large size, neither type of granule was of a shell structure with an empty interior. The R2 granules were rather uniform in structural appearance from the inside out (Fig. 1d). In comparison, the R1 granules had an apparently layered structure from the centre to the surface. No dark or black zones were found at the centre of the yellow R1 granules, thus signifying a non-anaerobic condition inside the large granules (Fig. 1c). This is rather remarkable, as an anaerobic condition is expected for the centre of a microbial granule as large as 20 mm due to the common DO transfer limitation. For aerobic granules, it has been reported that DO could penetrate only partially through 500 μm from the granule surface into the granules under a substrate-sufficient condition (Li et al., 2008b).

SEM microscopic examination revealed different microbial communities for the two types of large granules. The yellow granules in R1 were dominated by rod-shaped bacteria (Figs. 2a and 2b), and most of the bacterial cells were clustered together, with only a few filamentous microbial species found inside the granules. In contrast, the large black granules in R2 were primarily formed by fungi-like long filamentous cells (Figs. 2c and 2d).

3.2. Physical and physiological structures of the aerobic granules

The CLSM examination of the spatial distributions of the cells and EPS in the granules indicated different structural configurations for the two types of granules cultivated in R1 and R2. Based on the CLSM cryosections after fluorescent staining, the R1 granules were not empty inside, but had abundant bacterial cells towards their centres. In fact, there was a rather uniform distribution of bacterial cells and EPS throughout these granules (Figs. 3a-c). In contrast, filamentous cells were found to grow throughout the R2 granules, and EPS were present (Figs. 3d-f).

Closer CLSM examination revealed a web-like structure within the bacterial granules from R1 (Figs. 4a and 4b). Apparently, the bacteria were clustered together by EPS to build the members of the granules' web network. It has been suggested that gel-forming polysaccharides play an important role in the construction of a stable structure for aerobic granules (Yang et al., 2005; Wang et al., 2006). Large pores formed between the members of the granules' web structure, and many of these large pores were a few hundred μm in size, which would allow effective material transfers, including substrates and DO, into the interior of the granules. As a result, no anaerobic condition was observed at the centre of the large granules in which abundant bacterial growth was evidenced. In comparison, the fungal granules from R2 had a much looser and more porous configuration. The filamentous cells

and the bundles of the filaments tangled with one another to form a fluffy and loose granule structure (Figs. 4c and 4d).

3.3. Microbial communities for the two types of granules

For additional analysis, the granules were homogenised into cell mixtures in suspensions. The FISH-CLSM images of the cell mixtures indicated clearly different microbial communities for the two types of granules. Those from R1 were mainly composed of rod-shaped bacteria (Fig. 5a), although a few eukaryotes were also found (Fig. 5b). The granules from R2, in contrast, were dominated by filamentous eukaryal species (Fig. 5c), and some of the hyphae were attached to a few bacterial cells (Fig. 5d). According to area-based image analysis of the FISH images, bacteria accounted for approximately 84% of the microbial population in the R1 granules, whilst eukaryotes accounted for the remaining 17%. In comparison, the black R2 granules were approximately 84% eukaryotes and only 16% bacteria. This analysis confirmed that the high organic loading rate enhanced the growth of bacteria to form large bacterial granules in R1. Meanwhile, the low COD loading condition in R2 was unfavourable to such growth, but more favourable to fungi and other eukaryal species, thus leading to the formation of large filamentous granules.

The evolution in the microbial community during the formation of the special granules was indicated by the DGGE profiles. The DGGE band pattern of the bacteria in the large granules from R1 was largely different from that of the seed granules (Fig. 6), and at the high COD loading rate, this change in the DGGE profile was rather dynamic. Only four of the dominant bacterial bands (Bands 16, 18, 20 and 22) for the seed granules remained for the mature R1 granules after 120 d of cultivation.

To identify the bacterial DGGE bands of the R1 granules, they were compared with 24 OTUs selected from 98 clones in the library. The bands that did not match any of the OTUs

in the library were excised and sequenced for identification. Of the 31 bands that appeared in the DGGE profiles (Fig. 6), 22 dominant bands were identified (Table SM1 in Supplementary Material), accounting for > 85% of the total bacterial community of the R1 granules. The majority of the bacteria grouped with members of *Proteobacteria*, with three in the *Alphaproteobacteria*, nine in the *Betaproteobacteria*, and one in the *Gammaproteobacteria*. The next three groups clustered with *Flavobacteria*, followed by two with *Firmicutes*, two with *Sphingobacteria*, one with *Actinobacteria* and one with *Planctomycetes*.

Bacteria from the classes *Alphaproteobacteria* and *Betaproteobacteria* have commonly been found in conventional activated sludge (Bond et al., 1995; Snaidr et al., 1997; Vigeant et al., 2002). Bacteria from *Flavobacteria* have also been reported to be dominant in aerobic granules (Li et al., 2008a). After 120 d, Band 15, which corresponds to a close relative of *Acidovorax*, became dominant in R1, accounting for 25% of the total bacterial community judging from the DGGE band intensity. Bands 20 and 21, which were present as major bands during the entire process, were identified as *Riemerella anatipestifer* and *Pedobacter* sp., respectively. *Lactococcus* (Band 2), *Streptococcus* (Band 5) and *Flavobacterium* sp. (Band 9), which were less significant in the seed granules, became dominant (accounting for 4, 2 and 5%, respectively) in the mature R1 granules after 120 d.

The eukaryal DGGE band pattern for the black granules formed in R2 also indicated evolution in the eukaryal community during the growth process (Fig. 7). At a low COD loading rate of 0.5 g L^{-1} d^{-1}, however, the change of the eukaryal population structure was less dramatic. Most of the major bands could be found in both the seed granules and the large granules after 120 d of cultivation, although the positions of some of them had shifted during the process (Fig. 7).

Band 1 was identified as a *Cercozoa* species (Table SM2), a motile protist with a filose pseudopodal morphology. The protozoan phylum *Cercozoa* has been found to be a major

295 component of marine, freshwater and, especially, soil ecosystems. They are grazers that feed
296 on bacterial cells and detritus (Cavalier-Smith and Chao, 2003). Bands 2, 6 and 17 were
297 identified as *Geotrichum fragrans*, *Dipodascus ingens* and *Cochlonema euryblastum*,
298 respectively, all of which belong to *Fungi* and occurred in the seed granules. The microscopic
299 examinations indicated that fungal species were clearly the most important eukaryotes in the
300 large black granules in R2. *C. euryblastum*, however, disappeared from R2 after 120 d, and *D.*
301 *ingens* was always dominant. Band 11, *Epistylis urceolata*, also became more abundant in R2.
302 The genus *Epistylis* is a non-motile stalked ciliate similar to *Vorticella* that is common in
303 activated sludge, and *Cercozoa*, *G. fragrans* and *E. urceolata* have been found dominating in
304 aerobic filamentous granules (Williams and de los Reyes, 2006).
305
306 **4. Discussion**

307 It is generally believed that fungi are able to grow with an extremely low level of
308 nutrients and that it is wasteful to supply rich substrates (Deacon, 2006). Hence, fungal cells
309 may have an advantage over bacteria in substrate uptake under a low loading condition (such
310 as that in R2). A higher organic loading rate (such as that in R1), in contrast, allows bacterial
311 cells to outgrow fungal filaments in granules. When exposed to a high organic loading
312 condition at 2.0 g L^{-1} d^{-1}, the granules in R1 had an initial F/M ratio of 2.0 g COD g^{-1} SS d^{-1}.
313 This F/M ratio decreased gradually to around 0.8 g COD g^{-1} SS d^{-1} with granular biomass
314 growth. In R2, which was subject to a lower organic loading condition of 0.5 g L^{-1} d^{-1}, the
315 granules had an initial F/M ratio of 0.5 g COD g^{-1} SS d^{-1}, dropping gradually to about 0.2 g
316 COD g^{-1} SS d^{-1} with biomass growth. Thus, the granules in R1 always had a higher F/M ratio
317 that was around four times that of those in R2. As a result, large non-filamentous bacterial
318 granules stabilised in R1, in which the black filaments gradually disappeared (Fig. 1c). In R2,

319 there was a low F/M ratio, and the fungal filaments outgrew the bacteria to form large
320 filamentous granules (Fig. 1d).

321 The DGGE profiles for bacteria in R2 and eukaryal species in R1 during the experimental
322 process were also analysed (Fig. SM-1 and Fig. SM-2 in Supplementary Material). The two
323 reactors, R1 and R2, did not differ greatly in terms of the microbial diversity. However, the
324 main difference between the two reactors was the dominance of the microbial communities
325 by different types of species, although many other species were also present in the granules.
326 The granules in R1 were dominated by bacterial cells, whilst those in R2 were dominated by
327 fungal filaments (Fig 1, Fig. 5). This comparison between two batch reactors with the same
328 seed granules suggests that a higher organic loading condition helps non-filamentous bacteria
329 to out-compete filaments, whilst filamentous fungi become dominant under a low substrate
330 loading condition. It is apparent that bacterial granules that have deteriorated with fungal
331 growth can be recovered by increasing the organic loading rate. Some of these fungal
332 filaments may have had a few rod-shaped bacteria attached. Liu and Tay (2004) reported that
333 glucose-fed aerobic granules exhibited a loose morphology and were dominated by
334 filamentous bacteria. However, our previous experiments showed that, with proper pH
335 control to a level close to 8.0, a filamentous structure is unnecessary for the formation of
336 glucose-fed granules dominated by rod-shaped bacteria (Li et al., 2008a; Yang et al., 2008).
337 The present study suggests that, in addition to pH, the organic loading rate can also affect the
338 growth of dominant microbial species in aerobic sludge granules.

339 Despite the large size of the bacterial granules from R1, no anaerobic condition was
340 evidenced towards the granule centres, as no dark or black zones were found at the centre.
341 Under anaerobic conditions, sulphate-reducing bacteria would reduce sulphate to hydrogen
342 sulphide, which precipitates trace metals as metal sulphides with black colour (Peiffer, 1994;
343 Kaksonen et al., 2003). The large granules however had a special web-like structure in which

the bacteria were glued together by EPS to build the members of the web network. Large pores of a few hundred μm in size were formed between the members to allow effective substrate and DO transport into the interior of the granules for aerobic bacterial growth. Such a unique web structure has not previously been reported for microbial granules in biological wastewater treatment. For the black granules from R2, the filamentous fungi and other eukaryal species formed a much looser structure, and material transport limitation was less expected.

DNA-based molecular analysis indicated a rather dynamic evolution in the bacterial population within the R1 granules under a high organic loading condition. At the same time, the fungal bloom that occurred in the seed granules was effectively suppressed. At a low loading rate, the change of the eukaryal community structure in the R2 granules was less dynamic. Nonetheless, the fungal species outgrew the bacterial species in R2, thus transforming the yellow bacterial granules into black fungal granules. These experimental results suggest that the organic loading rate may be an important factor in the fate of aerobic bacterial granules that have deteriorated with fungal growth. A high organic loading condition helps to minimise the growth of filamentous species, restore bacterial domination and hence re-stabilise aerobic granules that suffer from deterioration caused by fungal bloom.

Acknowledgments

This research was supported by grants N-HKU737/04 and HKU7144/E07 from the Research Grants Council (RGC) of the Hong Kong SAR Government and grant 50828802 from the Natural Science Foundation of China. The technical assistance of Mr Keith C.H. Wong is highly appreciated.

References

APHA, 1998. Standard Methods for the Examination of Water and Wastewater. 20th ed. American Public Health Association, Washington D.C., USA.

Arrojo, B., Mosquera-Corral, A., Garrido, J.M., Mendez, R., 2004. Aerobic granulation with industrial wastewater in sequencing batch reactors. Water Res. 38, 3389-3399.

Beun, J.J., Hendriks, A., van Loosdrecht, M.C.M., Morgenroth, E., Wilderer, P.A., Heijnen, J.J., 1999. Aerobic granulation in a sequencing batch reactor. Water Res. 33, 2283-2290.

Bond, P.L., Hugenholtz, P., Keller, J., Blackall, L.L., 1995. Bacterial community structures of phosphate-removing and non-phosphate-removing activated sludges from sequencing batch reactors. Appl. Environ. Microb. 61, 1910-1916.

Cavalier-Smith, T., Chao, E.E.Y., 2003. Phylogeny of *Choanozoa*, *Apusozoa*, and other *Protozoa* and early *Eukaryote Megaevolution*. J. Mol. Evol. 56, 540-563.

Chu, H.P., Li, X.Y., 2005. Membrane fouling in a membrane bioreactor (MBR): Sludge cake formation and fouling characteristics. Biotechnol. Bioeng. 90, 323-331.

Deacon, J., 2006. Fungal Biology. 4th ed. Blackwell Publishing, Malden, MA, USA.

Diao, H.F., Li, X.Y., Gu, J.D., Shi, H.C., Xie, Z.M., 2004. Electron microscopic investigation of the bactericidal action of electrochemical disinfection in comparison with chlorination, ozonation and Fenton reaction. Process Biochem. 39, 1421-1426.

Diez, B., Pedros-Alio, C., Marsh, T.L., Massana, R., 2001. Application of Denaturing Gradient Gel Electrophoresis (DGGE) to study the diversity of marine picoeukaryotic assemblages and comparison of DGGE with other molecular techniques. Appl. Environ. Microb. 67, 2942-2951.

Eckenfelder, W.W., 2000. Industrial Water Pollution Control. 3th ed. McGraw-Hill, Singapore.

392 Kaksonen, A.H., Riekkola-Vanhanen, M.L., Puhakka, J.A., 2003. Optimization of metal
393 sulphide precipitation in fluidized-bed treatment of acidic wastewater. Water Res. 37,
394 255-266.
395 Knoop, S., Kunst, S., 1998. Influence of temperature and sludge loading on activated sludge
396 settling, especially on *Microthrix parvicella*. Water Sci. Technol. 37(4-5), 27-35.
397 Li, A.J., Yang, S.F., Li, X.Y., Gu, J.D., 2008a. Microbial population dynamics during aerobic
398 sludge granulation at different organic loading rates. Water Res. 42, 3552-3560.
399 Li, Y., Liu, Y., Shen, L., Chen, F., 2008b. DO diffusion profile in aerobic granule and its
400 microbiological implications. Enzyme Microb. Technol. 43,349-354.
401 Liu, B.B., Zhang, F., Feng, X.X., Liu, Y.D., Yan, X., Zhang, X.J., Wang, L.H., Zhao, L.P.,
402 2006. *Thauera* and *Azoarcus* as functionally important genera in a denitrifying
403 quinoline-removal bioreactor as revealed by microbial community structure comparison.
404 FEMS Microbiol. Ecol. 55, 274-286.
405 Liu, Y., Liu, Q.S., 2006. Causes and control of filamentous growth in aerobic granular sludge
406 sequencing batch reactors. Biotechnol. Adv. 24, 115-127.
407 Liu, Y., Tay, J.H., 2004. State of the art of biogranulation technology for wastewater
408 treatment. Biotechnol. Adv. 22, 533-563.
409 Liu, Y., Wang, Z.W., Qin, L., Liu, Y.Q., Tay, J.H., 2005. Selection pressure-driven aerobic
410 granulation in a sequencing batch reactor. Appl. Microbiol. Biot. 67, 26-32.
411 Morgenroth, E., Sherden, T., van Loosdrecht, M.C.M., Heijnen, J.J., Wilderer, P.A., 1997.
412 Aerobic granular sludge in a sequencing batch reactor. Water Res. 31, 3191-3194.
413 Muyzer, G., de Waal, E.C., Uitterlinden, A.G., 1993. Profiling of complex microbial
414 populations by denaturing gradient gel electrophoresis analysis of polymerase chain
415 reaction-amplified genes coding for 16S rRNA. Appl. Environ. Microb. 59, 695-700.

Peiffer, S., 1994. Predicting trace-metal speciation in sulphidic leachates from anaerobic solid-waste digestors by use of the pH_2S-value as a master variable. J. Contam. Hydrol. 16, 289-313.

Qin, L., Liu, Y., 2006. Aerobic granulation for organic carbon and nitrogen removal in alternating aerobic-anaerobic sequencing batch reactor. Chemosphere 63, 926-933.

Schwarzenbeck, N., Borges, J.M., Wilderer, P.A., 2005. Treatment of dairy effluents in an aerobic granular sludge sequencing batch reactor. Appl. Microbiol. Biot. 66, 711-718.

Snaidr, J., Amann, R., Huber, I., Ludwig, W., Schleifer, K.H., 1997. Phylogenetic analysis and *in situ* identification of bacteria in activated sludge. Appl. Environ. Microb. 63, 2884-2896.

Tay, J.H., Liu, Q.S., Liu, Y., 2001. Microscopic observation of aerobic granulation in sequential aerobic sludge blanket reactor. J. Appl. Microbiol. 91, 168-175.

Tay, J.H., Liu, Q.S., Liu, Y., 2002. Characteristics of aerobic granules grown on glucose and acetate in sequential aerobic sludge blanket reactors. Environ. Technol. 23, 931-936.

Vigeant, M.A.S, Ford, R.M., Wagner, M., Tamm, L.K., 2002. Reversible and irreversible adhesion of motile *Escherichia coli* cells analyzed by total internal reflection aqueous fluorescence microscopy. Appl. Environ. Microb. 68, 2794-2801.

Wang, Z.P., Liu, L.L., Yao, J., Cai, W.M., 2006. Effects of extracellular polymeric substances on aerobic granulation in sequencing batch reactors. Chemosphere 63, 1728-1735.

Watanabe, K., Teramoto, M., Futamata, H., Harayama, S., 1998. Molecular detection, isolation, and physiological characterization of functionally dominant phenol-degrading bacteria in activated sludge. Appl. Environ. Microb. 64, 4396-4402.

439 Weber, S.D., Wanner, G., Ludwig, W., Schleifer, K.H., Fried, J., 2007. Microbial
440 composition and structure of aerobic granular sewage biofilms. Appl. Environ. Microb.
441 73, 6233-6240.
442 Williams, J.C., de los Reyes, F.L., 2006. Microbial community structure of activated sludge
443 during aerobic granulation in an annular gap bioreactor. Water Sci. Technol. 54(1), 139-
444 146.
445 Yang, S.F., Li, X.Y., Yu, H.Q., 2008. Formation and characterisation of fungal and bacterial
446 granules under different feeding alkalinity and pH conditions. Process Biochem. 43, 8-
447 14.
448 Yang, S.F., Tay, J.H., Liu, Y., 2005. Effect of substrate nitrogen/chemical oxygen demand
449 ratio on the formation of aerobic granules. J. Environ. Eng. - ASCE 131, 86-92.
450 Zhang, T., Fang, H.H.P., 2004. Distribution of extracellular polysaccharides in the anaerobic
451 granular sludges, in: Ujang, Z., Henze, M. (Eds.), Water and Environmental
452 Management Series: Environmental Biotechnology. IWA publishing, London, UK, pp.
453 153-158.
454 Zhuang, W.Q., Tay, J.H., Yi, S., Tay, S.T.L., 2005. Microbial adaptation to biodegradation of
455 tert-butyl alcohol in a sequencing batch reactor. J. Biotechnol. 118, 45-53.
456

Figure captions

Fig. 1. Photographs of the aerobic granular sludge in the two batch reactors: (a) and (b) seed granules from a SBR and (c) large bacterial granules from R1 and (d) large fungal granules from R2, respectively, after 120 d of cultivation.

Fig. 2. SEM images of the microstructure of (a) and (b) mature granules from R1 and (c) and (d) mature granules from R2.

Fig. 3. CLSM images of the cryosections of the granules cultivated in (a-c) R1 and (d-f) R2. Depth: (a) 0.2 mm, (b) 3 mm, (c) 7 mm, (d) 3 mm; (e) 7 mm and (f) 12 mm. The cells were stained with SYTO9 (green) and the EPS polysaccharides with ConA-TRITC (red).

Fig. 4. CLSM images of the cryosections towards the centre of the granules from (a) and (b) R1 and from (c) and (d) R2. The cells were stained with SYTO9 (green) and the EPS polysaccharides with ConA-TRITC (red).

Fig. 5. FISH-CLSM images of the microbial cells in the granules from (a) and (b) R1 and from (c) and (d) R2. The bacteria were labelled by probe Eub338-FITC (green), and the fungi were shown to be eukaryal by probe Euk516-Cy3 (red).

Fig. 6. DGGE profiles and the abundance of the major bacterial species in the R1 granules during the growth process: (a) DGGE image, (b) DGGE schematic and (c) the relative abundance of the dominant bacterial species, as obtained through analysis of the DGGE banding profiles (SG - seed granules; d - days of batch cultivation).

Fig. 7. DGGE profiles and the abundance of the major eukaryal species in the R2 granules during the growth process: (a) DGGE image, (b) DGGE schematic and (c) the relative abundance of the dominant eukaryal species, as obtained through analysis of the DGGE banding profiles (SG - seed granules; d - days of the batch cultivation).

Figures

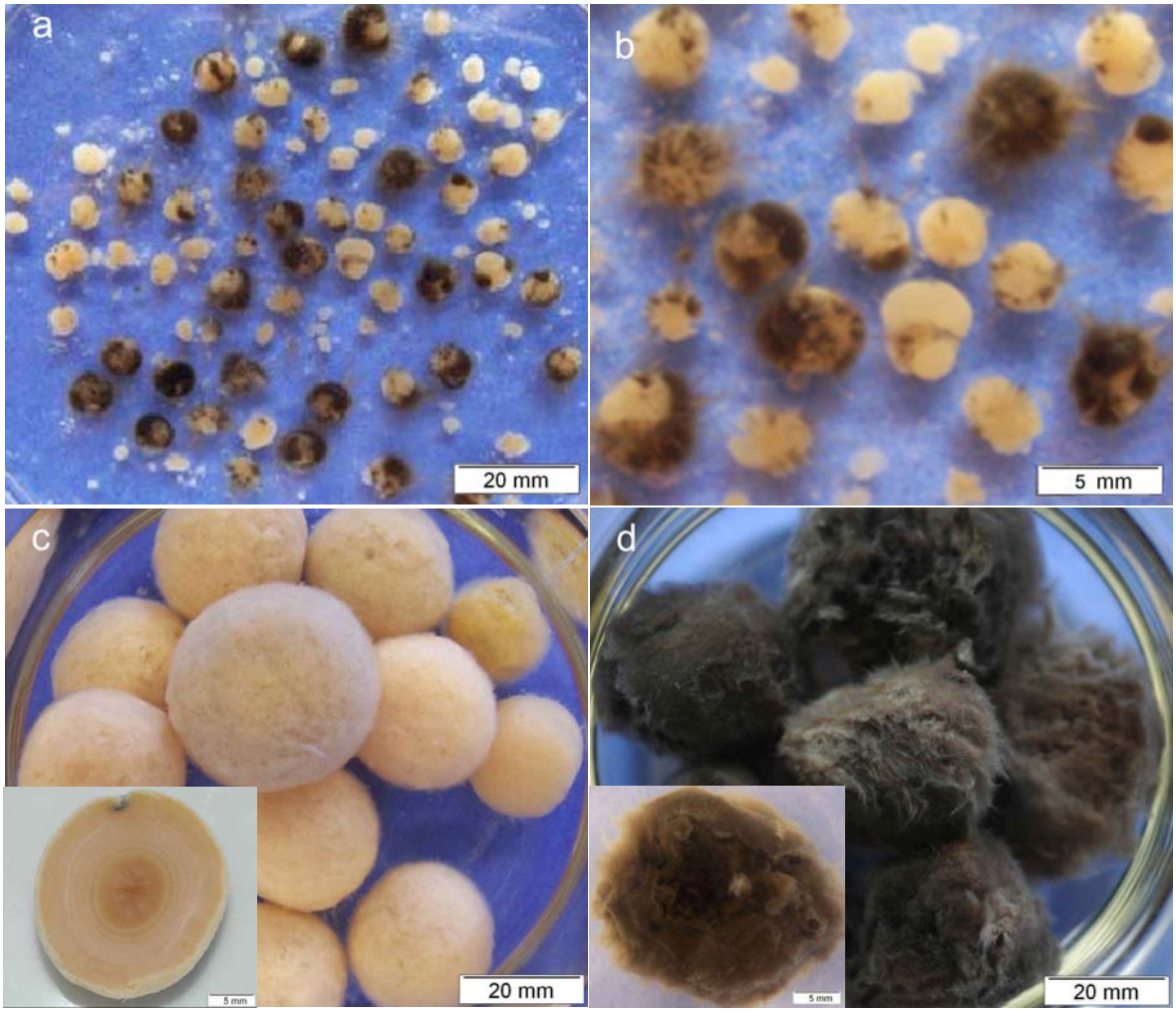

Fig. 1. Photographs of the aerobic granular sludge in the two batch reactors: (a) and (b) seed granules from a SBR and (c) large bacterial granules from R1 and (d) large fungal granules from R2, respectively, after 120 days of cultivation.

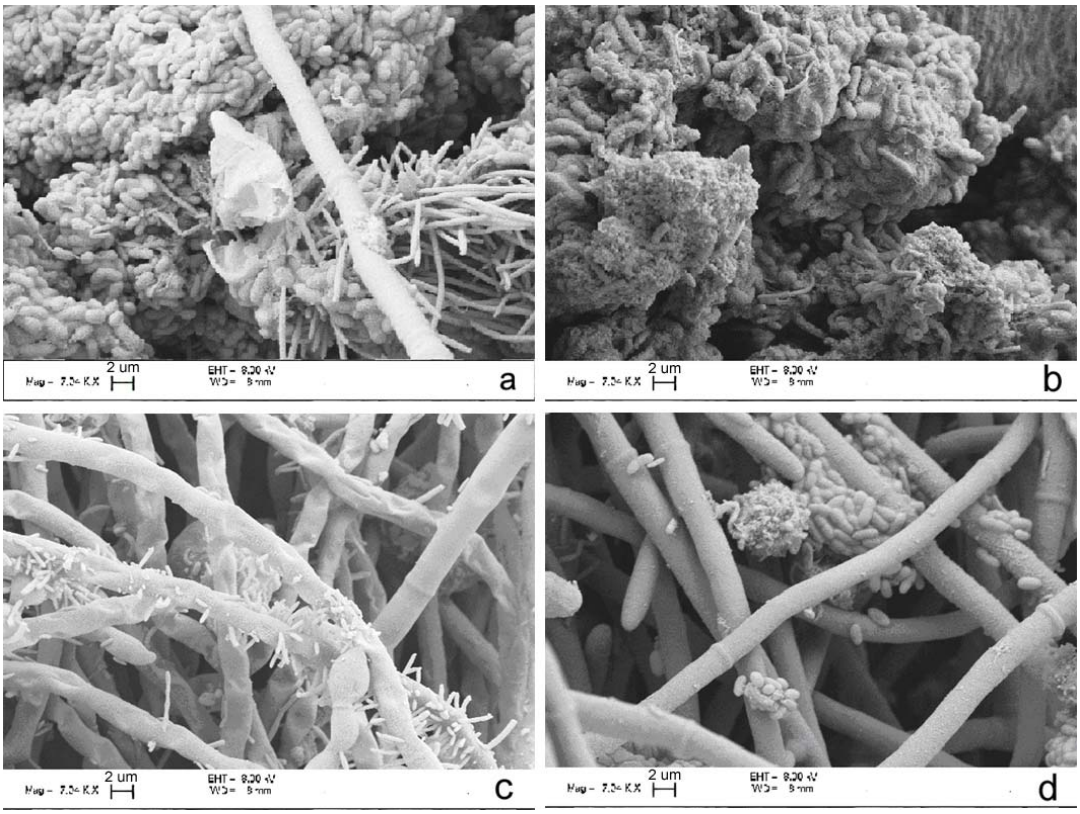

Fig. 2. SEM images of the microstructure of (a) and (b) mature granules from R1 and (c) and (d) mature granules from R2.

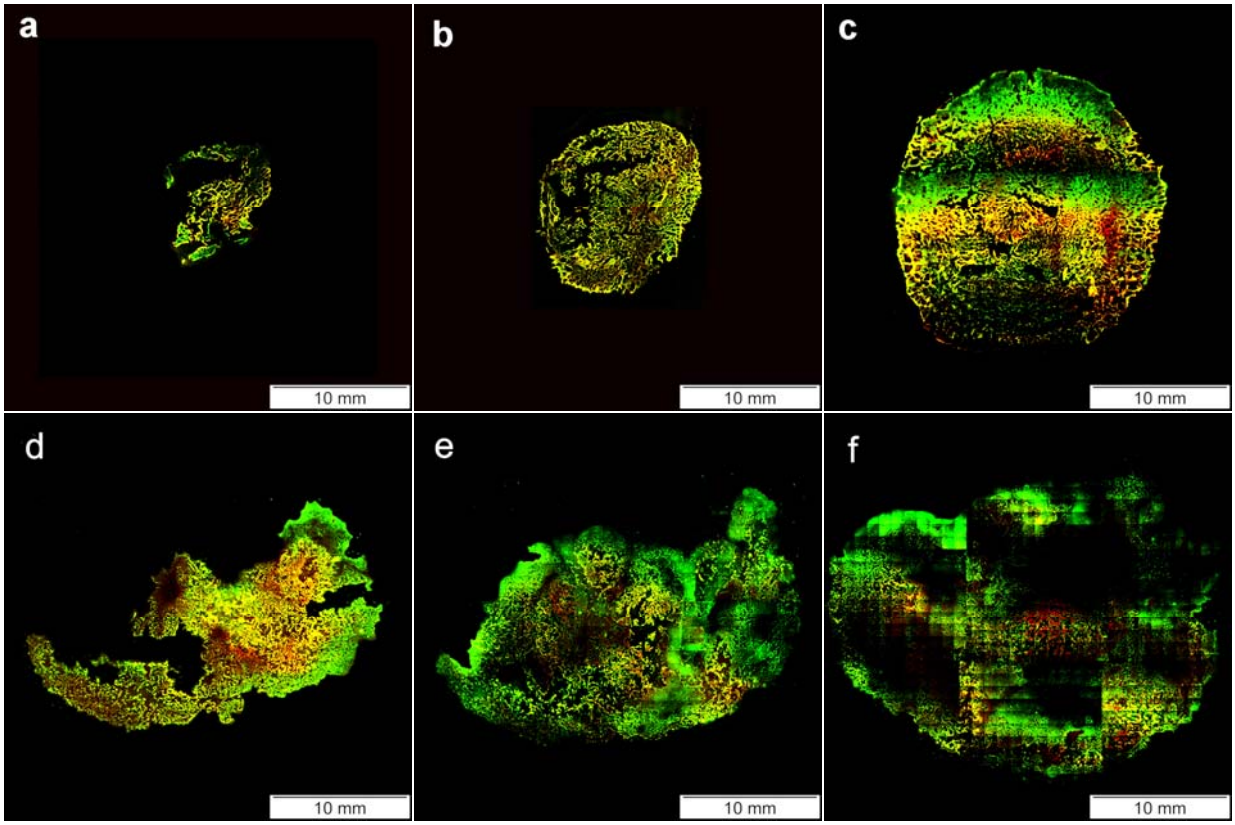

Fig. 3. CLSM images of the cryosections of the granules cultivated in (a-c) R1 and (d-f) R2. Depth: (a) 0.2 mm, (b) 3 mm, (c) 7 mm, (d) 3 mm; (e) 7 mm and (f) 12 mm. The cells were stained with SYTO9 (green) and the EPS polysaccharides with ConA-TRITC (red).

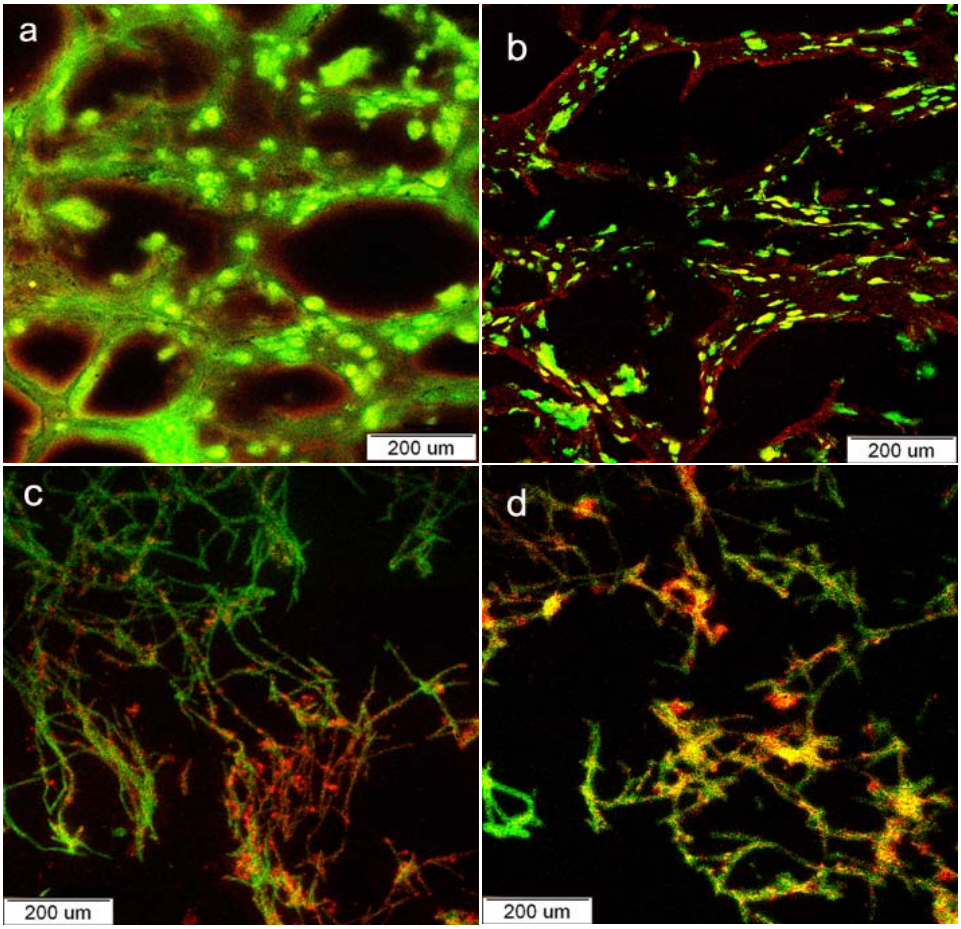

Fig. 4. CLSM images of the cryosections towards the centre of the granules from (a) and (b) R1 and from (c) and (d) R2. The cells were stained with SYTO9 (green) and the EPS polysaccharides with ConA-TRITC (red).

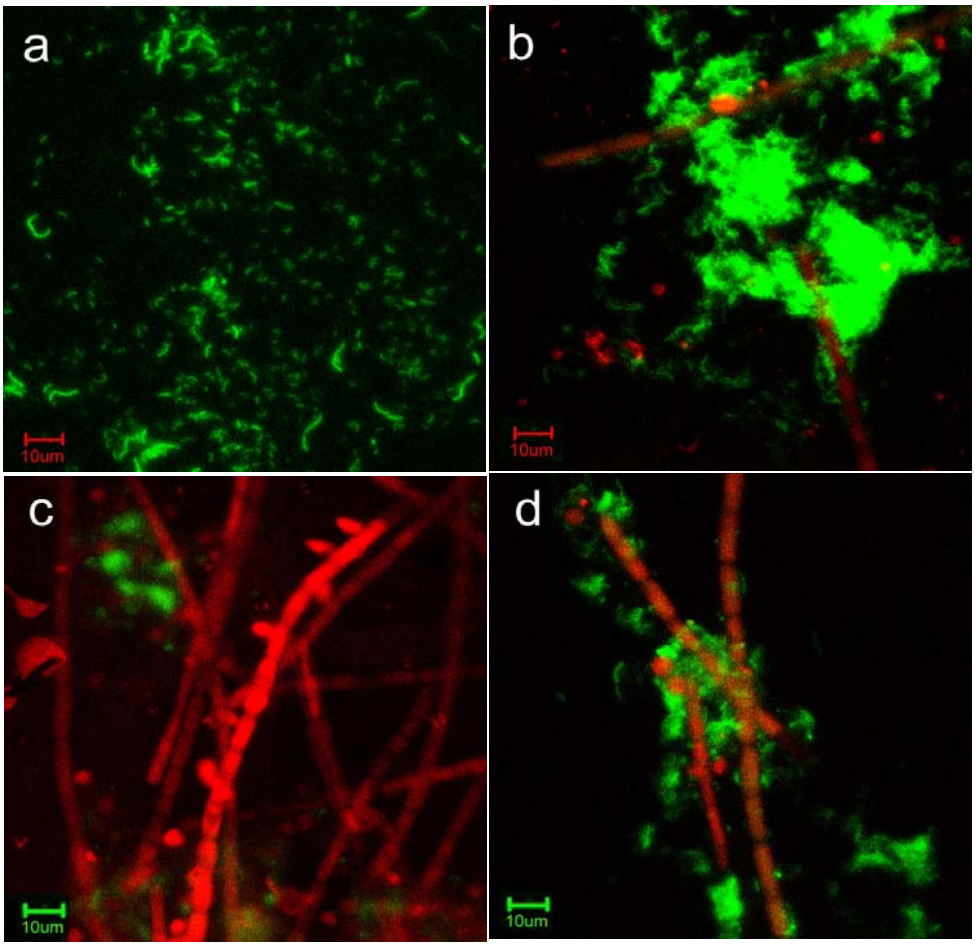

Fig. 5. FISH-CLSM images of the microbial cells in the granules from (a) and (b) R1 and from (c) and (d) R2. The bacteria were labelled by probe Eub338-FITC (green), and the fungi were shown to be eukaryal by probe Euk516-Cy3 (red).

(a)

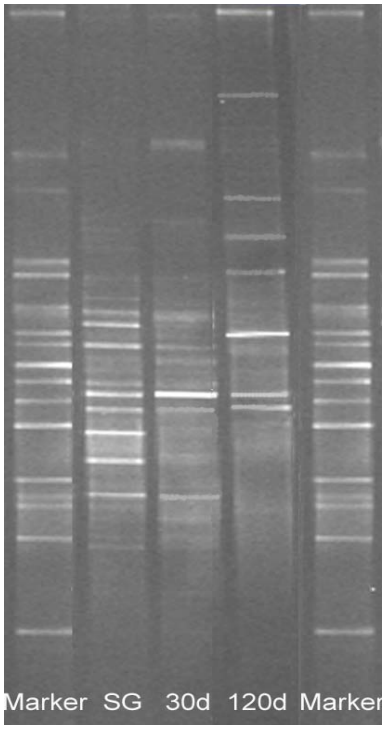

(b)

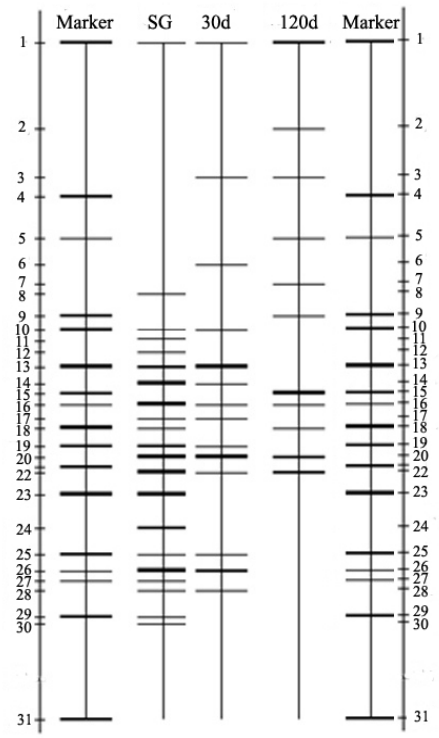

(c)

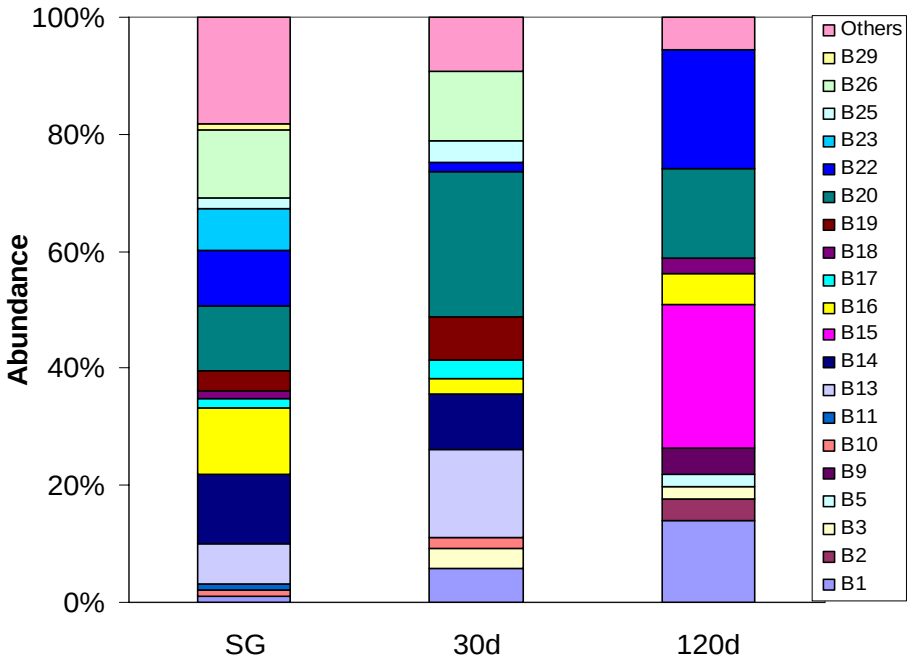

Fig. 6. DGGE profiles and the abundance of the major bacterial species in R1 granules during their growth process: (a) DGGE image, (b) DGGE schematic, and (c) the relative abundance of the dominant bacterial species as obtained from the analysis of the DGGE banding profiles (SG - seed granules, d - days of the batch cultivation).

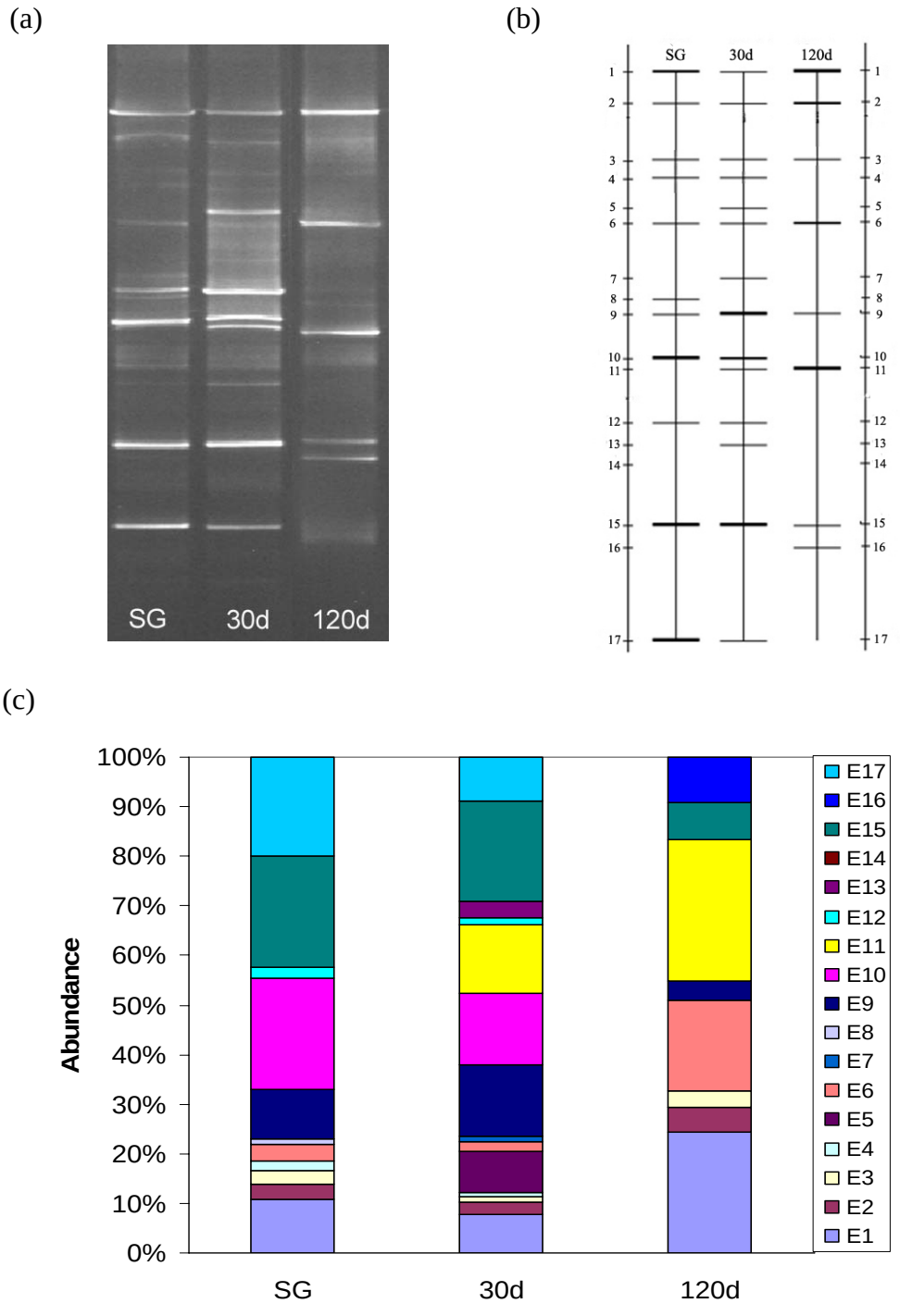

Fig. 7. DGGE profiles and the abundance of the major eukaryal species in the R2 granules during the growth process: (a) DGGE image, (b) DGGE schematic and (c) the relative abundance of the dominant eukaryal species, as obtained through analysis of the DGGE banding profiles (SG - seed granules; d - days of the batch cultivation).